Table of contents

for

Plasmon resonance light scattering assay of glucose based-on the formation of gold nanoparticles

Wen Bi Wu,[a] Lei Zhan,[b] Jian Wang[*a] and Cheng Zhi Huang[*a,b]

[a] *College of Pharmaceutical Science, Southwest University, Chongqing 400716, China. Fax:*

(+86) 23 68367257; Tel: (+86) 23 68254659; E-mail: wj123456@swu.edu.cn;

chengzhi@swu.edu.cn

[b] *Key Laboratory of Luminescent and Real-Time Analytical Chemistry (Southwest University）,*

Ministry of Education, College of Chemistry and Chemical Engineering, Southwest University,

Chongqing 400715, China
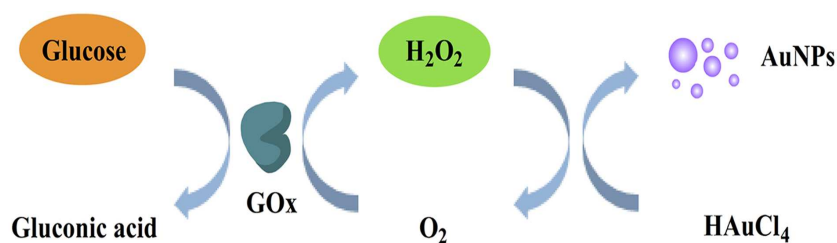
RLS assay for glucose based on the formation of AuNPs by coupling redox H_2O_2 of with biocatalytic reaction of GOx.

PAPER

Plasmon resonance light scattering assay of glucose based-on the formation of gold nanoparticles

Wen Bi Wu,[a] **Lei Zhan,**[b] **Jian Wang*[a] and Cheng Zhi Huang*[a,b]**

A simple and label-free plasmon resonance light scattering (PRLS) assay for glucose was developed based on the formation of gold nanoparticles (AuNPs) from the redox between chlorauric acid (HAuCl$_4$) and hydrogen peroxide (H$_2$O$_2$) in the presence of MES. It was found the PRLS signals characterized at 550 nm were proportional to the content of H$_2$O$_2$, which could be produced in the process of biocatalytic
10 reaction of glucose oxidase (GOx), and thus a RLS method of glucose was proposed with the linear range of 5.0×10^{-6} M to 1.0×10^{-4} M and detection limit of 2.7×10^{-6} M.

1. Introduction

In recent years, metal nanoparticles have been intensely studied for applications in investigations of DNA hybridization,[1, 2]
15 immunoassay[3, 4] and cellular imaging[5, 6] due to their peculiar physical and chemical properties, which are not present in bulk materials.[7] Specifically, the localized surface plasmon resonance (LSPR), which strongly depends on the shape, size and aggregation of nanoparticles, is of great interest to scientists.
20 LSPR, including plasmon resonance absorption (PRA) and plasmon resonance light scattering (PRLS),[8, 9] is known to originate from the excitation of the collective oscillations of conducting electrons.[8] When a metal nanoparticle is exposed to the irradiation of light, plasmon resonance occurs with coherent
25 oscillation of the conduction electrons. Subsequently, the oscillating electrons radiate electromagnetic radiation with the same frequency as that of the oscillating electrons, and the radiation is often referred to as resonance light scattering (RLS).[9] As a powerful tool with distinct advantages of simplicity,
30 rapidness and high sensitivity, RLS technique has been widely applied for the determination of proteins,[10, 11] nucleic acids,[12, 13] drugs,[14, 15] chemical dyes,[16] metal ions,[17] and so on. As an example of metallic particles, nanoparticles such as gold nanoparticles (AuNPs) exhibit characteristic RLS signals in the
35 corresponding plasmon resonance absorption region, which have showed significant potential for biomolecular detection.

Hydrogen peroxide (H$_2$O$_2$) is an important metabolite of organisms that can be generated by many oxidative biological reactions, including those of glucose oxidase (GOx), uricase,
40 galactose oxidase, cholesterol oxidase, sarcosine oxidase, alcohol oxidase, and xanthine oxidase.[18, 19] And many analytical methods have been developed for detection of H$_2$O$_2$ and the respective substrates, such as chromatography,[20] electroanalysis,[21, 22] fluorometry,[23, 24] spectrophotometry[25] and RLS assays.[26] In
45 conventional colorimetric detection of H$_2$O$_2$ and glucose, signal is often generated by the conversion of substrate 3,3,5,5-tetramethylbenzidine (TMB) into a colourful molecule based on

the catalysis of peroxidase enzymes.[25] However, such natural enzymes are often expensive and their catalytic activity can be
50 easily inhibited,[27] thus severely limit the applications of these methods. Herein, we report a label-free RLS assay for glucose based on the formation of AuNPs instead of the catalyzation of peroxidase enzymes (Scheme 1). GOx generates H$_2$O$_2$ upon the catalytic oxidation of glucose, and H$_2$O$_2$ can be used to reduce
55 HAuCl$_4$ to form AuNPs in presence of MES (2-(4-morpholino) ethanesulfonic acid) under mild condition. Based upon the strong RLS signal of AuNPs, we can perform quantitative detection of glucose without any modification under mild condition.
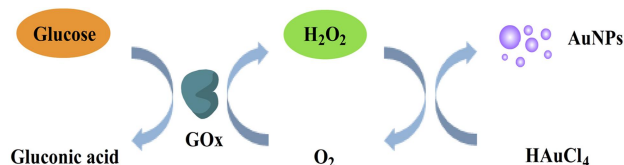
60 **Scheme 1** Schematic representation of the formation of AuNPs for RLS assay of glucose.

2. Experimental

2.1 Materials

GOx was purchased from Sigma–Aldrich (St. Louis, MO), which
65 was of 195.7 U mg^{-1} of lyophilized solid. HAuCl$_4$·H$_2$O was purchased from Sinopharm Group Chemical Regent Co., Ltd. (Shanghai, China). MES was purchased from Beijing Dingguo Changsheng Biotechnology Co., Ltd. (Beijing, China). H$_2$O$_2$, glucose, fructose, lactose, and maltose were obtained from
70 Chongqing Pharmaceutical Co., Ltd (Chongqing, China). The stock solution of H$_2$O$_2$ was diluted from 30% solution and the H$_2$O$_2$ standard solution was standardized by KMnO$_4$ titration. All reagents used in this work were of analytical grade without further purification, and Mili-Q purified water (18.2 MΩ) was
75 used throughout the experiment.

2.2 Apparatus

UV-vis spectra were recorded on a U-3010 spectrophotometer (Hitachi, Tokyo, Japan). The RLS spectra were measured with an F-4500 spectrofluorometer (Hitachi, Tokyo, Japan). The scanning electron microscopy (SEM) images of AuNPs were performed with an S-4800 scanning electron microscope (Hitachi, Tokyo, Japan) operating at 30.0 kV.

2.3 Procedure for H_2O_2

Various concentrations of H_2O_2 were incubated with $HAuCl_4$ (0.1 mM) in the presence of 10 mM PB buffer (pH 7.4) and 0.5 mM MES for 20 minutes at 25 ^{o}C. Subsequently, the mixture was immediately transferred for absorption, RLS and SEM measurements.

2.4 Procedure for glucose

Different concentrations of glucose were incubated with 50 μL GOx (0.1 mg mL^{-1}) in the presence of 10 mM PB buffer (pH 7.4) and 0.5 mM MES at 37 ^{o}C for 30 minutes. Then $HAuCl_4$ (0.1 mM) was added to the above reaction solution. After incubating at 25 ^{o}C for 20 minutes, the mixed solution was finally used to perform absorption and RLS measurements. To evaluate the specificity of this method, fructose, lactose, and maltose instead of glucose were used for the control experiments.

3. Results and discussion

3.1 The formation of AuNPs
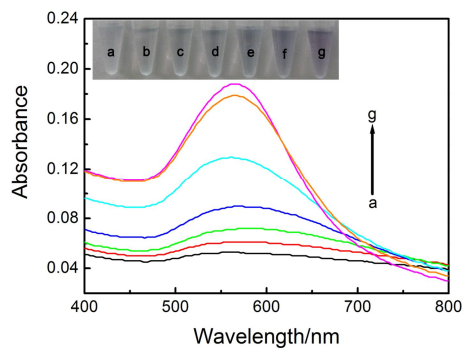
Fig. 1 UV-vis absorption spectra of AuNPs obtained at different concentrations of H_2O_2. The inset photograph shows the color changes of the solution. c_{HAuCl4}, 0.1 mM; c_{H2O2} (a to g), 0, 5, 15, 25, 50, 75, 100 μM; c_{MES}, 0.5 mM; c_{PB}, 10 mM, pH 7.4.

As a reactive oxygen species, H_2O_2 can not only be a strong oxidative agent[28] but also function as a reduction agent. Recently, the conversion of tetrachloroaurate ions into AuNPs using H_2O_2 as an alternative reducing agent has been reported.[29] The proposed reaction equation is

$$AuCl_4^- + \frac{3}{2}H_2O_2 \rightarrow Au^0 + 4Cl^- + 3H^+ + \frac{3}{2}O_2$$
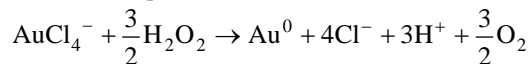
MES is also reported to be a mild reducing agent that can reduce the gold salt and stabilize newly formed gold nanostructures.[30, 31] Here, we take MES as a synergist to accelerate the formation of AuNPs. Since the concentration of MES is constant in all experiments, the concentration of H_2O_2 is the key factor that influences the formation of AuNPs.

To confirm the formation of AuNPs in the presence of H_2O_2, we first observed the absorption spectra of the product solutions. Fig.1 showed the generation of AuNPs in the presence of various concentrations of H_2O_2. When there was no H_2O_2, the solution showed a broad and weak absorption peak over the range of 450-800 nm. The results indicated that MES alone could lead to the formation of a few amorphous gold aggregates, which was identical with the previous reports.[30, 32] Furthermore, the addition of H_2O_2 to $HAuCl_4$ resulted in the increase of the absorbance, indicating the formation of a larger number of AuNPs. As the concentration of H_2O_2 increased, the characteristic plasmon absorbance of AuNPs was enhanced gradually. And the absorbance of AuNPs at about 560 nm showed a linear relationship with the concentration of H_2O_2 over the range of 5.0×10^{-6} M to 1.0×10^{-4} M (Fig. S1, ESI†).

3.2 RLS of the formed AuNPs
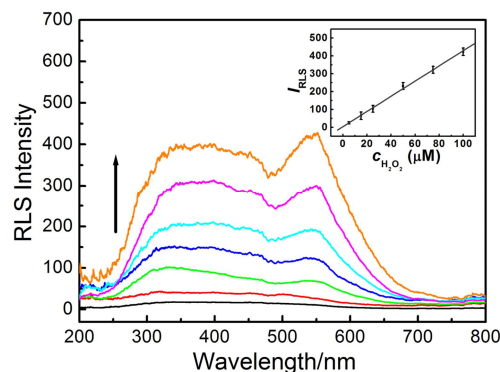

Fig. 2 RLS spectra of AuNPs obtained via the reduction of $HAuCl_4$. c_{HAuCl4}, 0.1 mM; c_{H2O2} (a to g), 0, 5, 15, 25, 50, 75, 100 μM; c_{MES}, 0.5 mM; c_{PB}, 10 mM, pH 7.4. The inset is linear plots corresponding to the RLS intensity at 550nm vs. the concentration of H_2O_2. The error bars represent the standard deviation of three measurements.

To further validate the formation of gold nanostructures, an experiment focusing on the RLS spectra was performed (Fig. 2).The product solutions obtained at different concentrations of H_2O_2 exhibited broad light scattering bands from 250 nm to 470 nm and light scattering peaks located at about 550 nm. It has been reported that the RLS effect could be observed in the absorption region of metal nanoparticles.[33, 34] Therefore, the characteristic light scattering peak at 550nm, which was corresponding to the plasmon absorption band around 560nm of AuNPs (Fig. 1), should be ascribed to the RLS signal of AuNPs.[35] And the broad light scattering band should be ascribed to the Rayleigh light scattering of the aqueous solution using an uncorrected spectrofluorometer.[34] The RLS signal was very weak when there was no H_2O_2. Upon treatment with H_2O_2, the intensity of scattering peaks was enhanced gradually with increasing H_2O_2 concentration, suggesting more AuNPs were formed.

It was found that the RLS intensity of the formed AuNPs was proportional to the concentration of H_2O_2, which could be applied for the quantification of H_2O_2. The insert in Fig. 3 showed the RLS intensity of AuNPs plotted against the concentration of H_2O_2. There was a good linear relationship between the RLS intensity and the concentration of H_2O_2 over the range of 5.0×10^{-6} M to 1.0×10^{-4} M with the detection limit of 2.4×10^{-6} M. The linear equation could be expressed as $I = 4.3c + 3.4$ (r, 0.9993), where I was the RLS intensity and c (μM) was the concentration of H_2O_2.

To understand the impact of the concentration of H_2O_2 on

the morphology and state of aggregation of AuNPs, we have performed further investigations of nanoparticle solutions by SEM inspection. Fig. 3 showed the SEM images of nanoparticles grown with H_2O_2 at concentrations of 5 µM (A) and 100 µM (B). For the low concentration of H_2O_2, a few ill-defined AuNPs aggregates were obtained. On the contrary, fewer aggregates of AuNPs and more quasi-spherical, non-aggregated AuNPs together with small crystalline AuNPs were formed at a higher H_2O_2 concentration. The results were identical with the absorption spectra (Fig. 1). A blue shift in the absorbance maxima with the concomitant absorbance growth was observed with the increasing concentration of H_2O_2. The blue shift should be ascribed to the mixture of different sized particles and the high absorbance features should be due to the increased content of AuNPs, which may imply the formation of more AuNPs of lower dimensions. Taken together, the results indicated that with the increasing H_2O_2 concentration, the number of formed AuNPs increased whereas the particle size or the state of aggregation decreased. On the one hand, the concentration of H_2O_2 was related with the kinetics of crystal growth. At a high H_2O_2 concentration, the reduction of gold salt by H_2O_2 occured at a fast rate to form more non-aggregated AuNPs while the reaction rate was relatively slow at a low H_2O_2 concentration to generate more aggregated nanoparticles.[31, 36] On the other hand, the more H_2O_2 added, the more reactant ($HAuCl_4$) was consumed, which contributed to the increasing number of AuNPs.[36, 37]
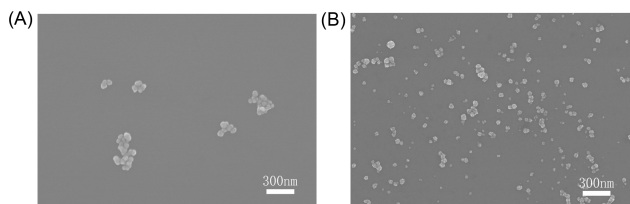

Fig. 3 SEM images of nanoparticles grown with H_2O_2 at concentrations of (A) 5 µM and (B) 100 µM. c_{HAuCl4}, 0.1 mM; c_{MES}, 0.5 mM; c_{PB}, 10 mM, pH 7.4.

In general, the light scattering property depends on the volume and number of the particles, the incident light wavelength, and the surrounding medium.[33, 34, 38] In this study, the enhanced light scattering intensity results from combined effect of the number and size of AuNPs. The increased number of AuNPs would lead to stronger light scattering signals while the decreased aggregation state or size of AuNPs would result in reduced light scattering signals. When the concentration of H_2O_2 is in the range of $5.0×10^{-6}$ M to $1.0×10^{-4}$ M, the increase of number is more obvious than the decrease of size, and the former has a greater impact on the RLS signals than the latter, thus the integrative effect of the two leads to the enhancement of light scattering signals. However, when the concentration of H_2O_2 is higher, more and more tiny crystalline AuNPs are formed, which exhibit much weak light scattering[38] and then results in the nonlinear response. Therefore, we can develop a RLS assay for substrates which could generate H_2O_2 based upon the using of the corresponding oxidases.

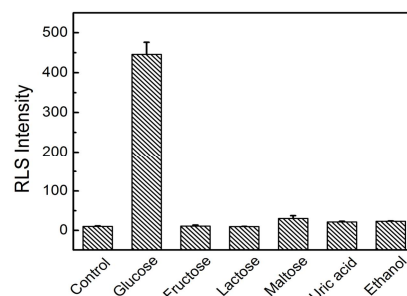### 3.3 Detection for glucose

GOx is generally acknowledged to catalyze the oxidation of glucose to gluconic acid and H_2O_2.[39] We further extended the above approach for glucose by coupling the formation of nanoparticles with glucose oxidation reaction. And the concentration of GOx was optimized to ensure that glucose was completely oxidized to H_2O_2 (Fig. S2, ESI†). Similar to the case of H_2O_2, the nanoparticle solutions showed an absorbance peak at about 560 nm (Fig. S3(A), ESI†), which could be ascribed to the plasmon resonance absorption of AuNPs. The absorbance got enhanced as the concentrations of glucose were elevated. Fig. 4 (A) showed the evolution of the measured light scattering spectra in the presence of variable concentrations of glucose. As shown, the nanoparticle solutions exhibited a broad light scattering band from 250 nm to 470 nm and a light scattering peak located at about 550 nm, which should be ascribed to the light scattering signal of the aqueous solution and AuNPs, respectively. And the results revealed a gradual increase of the RLS intensity upon increasing the concentration of glucose. As the concentration of glucose increases, the concentration of the generated H_2O_2 gets higher, this then results in the enhanced RLS and absorption signal.
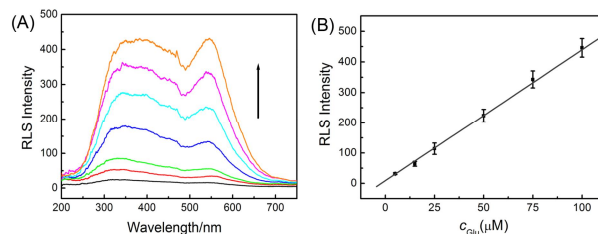
Fig. 4 (A) RLS spectra of AuNPs generated by the reduction of H_2O_2. $c_{glucose}$ (from bottom to up): 0, 5, 15, 25 ,50, 75, 100µM; c_{GOx}, 25µg mL^{-1}; c_{HAuCl4}, 0.1 mM; c_{MES}, 0.5 mM; c_{PB}, 10 mM, pH 7.4. (B) Linear plots between the RLS intensity at 550 nm and the concentration of glucose. The error bars represent the standard deviation of three measurements.

Fig. 5 Selectivity for glucose detection. $c_{glucose}$, 0.1 mM; $c_{fructose}$, 1 mM; $c_{lactose}$, 1 mM; $c_{maltose}$, 1 mM; $c_{uric\ acid}$, 1 mM; $c_{ethanol}$, 1 mM. c_{GOx}, 25µg mL^{-1}; c_{HAuCl4}, 0.1 mM; c_{MES}, 0.5 mM; c_{PB}, 10 mM, pH 7.4. The error bars represent the standard deviation of three measurements.

To determine the sensitivity of the method for glucose detection, various concentrations of glucose were added to $HAuCl_4$ in the presence of MES. Fig. 4 (B) showed the calibration curve of the RLS intensity at 550 nm versus the concentration of glucose. The linear range was from $5.0×10^{-6}$ M to $1.0×10^{-4}$ M and LOD was $2.7×10^{-6}$ M with the linear equation $I = 4.3c + 9.0$ (r, 0.9979), where I was the RLS intensity and c (µM) was the concentration of glucose. Besides, a good linear relationship between the absorbance at 560 nm and the concentration of glucose was also obtained in the range of $5.0×10^{-6}$ M to $1.0×10^{-4}$ M (Fig. S3(B), ESI†).

The influence of NaCl on the RLS intensity was tested. NaCl can be allowed to be lower than $2×10^{-6}$ M given the

tolerance of 10%, which is possibly due to its effect on the aggregation of nanoparticles. Meanwhile, to assess the specificity of the method, the influences of some glucose analogues as well as some common interferents such as uric acid and ethanol, were examined in aqueous buffer and the results were shown in Fig. 5. It can be seen that the RLS intensity only increased for glucose, which could be attributed to the high affinity of GOx to oxidized glucose.[40] Even when fructose, lactose, maltose, uric acid and ethanol were used at concentrations as high as 1 mM, the RLS signal remained as low as the background signal. The results have demonstrated that this method is of great selectivity for glucose detection. All the data above show that this method we developed is simple, fast, and sensitive for glucose detection.

4. Conclusions

In conclusion, a label-free RLS assay was proposed for glucose based on the formation of AuNPs with a common spectrofluorometer. While MES works as a synergistic reducing and stabilize agent, H_2O_2 can reduce gold salt into AuNPs. The formed AuNPs exhibit characteristic RLS signals at 550nm, which are proportional to the concentration of H_2O_2. By coupling biocatalytic reaction of GOx, we further develop a low-cost, simple, rapid and sensitive method for glucose. Furthermore, since many kinds of oxidases generate H_2O_2, it may also be a valuable approach for detection of other substrates.

Notes and references

a Key Laboratory of Luminescent and Real-Time Analytical Chemistry (Southwest University), Ministry of Education ,College of Pharmaceutical Sciences, Southwest University, Chongqing 400716, China. Fax: (+86) 23 68367257; Tel: (+86) 23 68254659; E-mail: wj123456@swu.edu.cn; chengzhi@swu.edu.cn
b College of Chemistry and Chemical Engineering, Southwest University, Chongqing 400715, China
† Electronic Supplementary Information (ESI) available: [details of any supplementary information available should be included here]. See DOI: 10.1039/b000000x/

1. R. C. Mucic, J. J. Storhoff, C. A. Mirkin and R. L. Letsinger, *J. Am. Chem. Soc.*, 1998, **120**, 12674-12675.
2. J. J. Storhoff and C. A. Mirkin, *Chem. Rev.*, 1999, **99**, 1849-1862.
3. A. F. Robson, T. R. Hupp, F. Lickiss, K. L. Ball, K. Faulds and D. Graham, *Proc. Natl. Acad. Sci. U. S. A*, 2012, **109**, 8073-8078.
4. J. Ling, Y. F. Li and C. Z. Huang, *Anal. Chem.*, 2009, **81**, 1707-1714.
5. L. Q. Chen, S. J. Xiao, P. P. Hu, L. Peng, J. Ma, L. F. Luo, Y. F. Li and C. Z. Huang, *Anal. Chem.*, 2012, **84**, 3099-3110.
6. X. Huang, I. H. El-Sayed, W. Qian and M. A. El-Sayed, *J. Am. Chem. Soc.*, 2006, **128**, 2115-2120.
7. S. Link and M. A. El-Sayed, *Int. Rev. Phys. Chem.*, 2000, **19**, 409-453.
8. K. L. Kelly, E. Coronado, L. L. Zhao and G. C. Schatz, *J. Phys. Chem. B*, 2003, **107**, 668-677.
9. K. Aslan, P. Holley, L. Davies, J. R. Lakowicz and C. D. Geddes, *J. Am. Chem. Soc.*, 2005, **127**, 12115-12121.
10. K. X. Zhang and X. L. Shen, *Analyst*, 2013, **138**, 1828-1834.
11. C. Z. Huang and Y. F. Li, *Anal. Chim. Acta*, 2003, **500**, 105-117.
12. X. Chen, G. L. Liu, S. W. Liang, S. H. Qian, J. B. Liu and Z. G. Chen, *Anal. Methods*, 2012, **4**, 1546-1551.
13. W. Lu, C. Z. Huang and Y. F. Li, *Analyst*, 2002, **127**, 1392-1396.
14. P. Feng, W. Q. Shu, C. Z. Huang and Y. F. Li, *Anal. Chem.*, 2001, **73**, 4307-4312.
15. Z. De Liu, C. Z. Huang, Y. F. Li and Y. F. Long, *Anal. Chim. Acta*, 2006, **577**, 244-249.
16. L. P. Wu, Y. F. Li, C. Z. Huang and Q. Zhang, *Anal. Chem.*, 2006, **78**, 5570-5577.
17. W. Qi, Y. Wang, J. Wang and C. Huang, *Sci China Chem.*, 2012, **55**, 1445-1450.
18. R. Liu, S. Li, X. Yu, G. Zhang, S. Zhang, J. Yao, B. Keita, L. Nadjo and L. Zhi, *Small*, 2012, **8**, 1398-1406.
19. J. Marangon, H. D. Correia, C. D. Brondino, J. J. Moura, M. J. Romao, P. J. Gonzalez and T. Santos-Silva, *PloS one*, 2013, **8**, e83234.
20. K. Wang and W. H. Glaze, *J. Chromatogr. A*, 1998, **822**, 207-213.
21. T. Ito, M. Kunimatsu, S. Kaneko, Y. Hirabayashi, M. Soga, Y. Agawa and K. Suzuki, *Talanta*, 2012, **99**, 865-870.
22. S. D. Sun, X. Z. Zhang, Y. X. Sun, J. Zhang, S. C. Yang, X. P. Song and Z. M. Yang, *RSC Advances*, 2013, **3**, 13712-13719.
23. X. Shu, Y. Chen, H. Yuan, S. Gao and D. Xiao, *Anal. Chem.*, 2007, **79**, 3695-3702.
24. X. D. Xia, Y. F. Long and J. X. Wang, *Anal. Chim. Acta*, 2013, **772**, 81-86.
25. Y. Jv, B. Li and R. Cao, *Chem. Commun.*, 2010, **46**, 8017-8019.
26. L. Shang, H. Chen, L. Deng and S. Dong, *Biosens. Bioelectron.*, 2008, **23**, 1180-1184.
27. E. Shoji and M. S. Freund, *J. Am. Chem. Soc.*, 2001, **123**, 3383-3384.
28. Q. Zhang, N. Li, J. Goebl, Z. Lu and Y. Yin, *J. Am. Chem. Soc.*, 2011, **133**, 18931-18939.
29. T. KumaráSarma, *Chem. Commun.*, 2002, **21**, 1048-1049.
30. C. Engelbrekt, K. H. Sørensen, J. Zhang, A. C. Welinder, P. S. Jensen and J. Ulstrup, *J. Mater. Chem.*, 2009, **19**, 7839-7847.
31. R. d. l. Rica and M. M. Stevens, *Nat. Nanotechnol.*, 2012, **7**, 821-824.
32. P. Gobbo, M. J. Biondi, J. J. Feld and M. S. Workentin, *J. Mater. Chem. B*, 2013, **1**, 4048-4051.
33. R. F. Pasternack, C. Bustamante, P. J. Collings, A. Giannetto and E. J. Gibbs, *J. Am. Chem. Soc.*, 1993, **115**, 5393-5399.
34. R. F. Pasternack and P. J. Collings, *Science*, 1995, **269**, 935-935.
35. B. A. Du, Z. P. Li and C. H. Liu, *Angew. Chem. Int. Ed.*, 2006, **45**, 8022-8025.
36. K. Pacławski and K. Fitzner, *Metal. Mater. Trans. B*, 2006, **37**, 703-714.
37. B. R. Panda and A. Chattopadhyay, *J. Nanosci. Nanotechnol.*, 2007, **7**, 1911-1915.
38. C. Z. Huang, K. A. Li and S. Y. Tong, *Anal. Chem.*, 1997, **69**, 514-520.
39. J. Rogalski, J. Fiedurek, J. Szczordrak, K. Kapusta and A. Leonowicz, *Enzyme Microb. Technol.*, 1988, **10**, 508-511.
40. R. Gill, L. Bahshi, R. Freeman and I. Willner, *Angew. Chem. Int. Ed.*, 2008, **120**, 1700-1703.